Journal of
Computational and Theoretical Nanoscience
Vol. 6, 1–5, 2008

Capacitive Effects in a Three-Terminal Organic Nano-Device

Marcos Allan Leite Reis[1], Aldilene Saraiva-Souza[2], and Jordan Del Nero[3,*]

[1] *Pós-graduação em Engenharia Elétrica, Universidade Federal do Pará, 66075-900, Belém, Pará, Brazil*
[2] *Pós-graduação em Física, Universidade Federal do Ceará, 60455-900, Fortaleza, Ceará, Brazil*
[3] *Departamento de Física, Universidade Federal do Pará, 66075-110, Belém, Pará, Brazil*

The investigation of nanodevices with specific capacitive effects is one of the issues that must be addressed to develop the nanotechnology subject. In this paper we present by quantum mechanics calculations, the design of these properties of an organic three-terminal nanodevice, the controlled molecular rectifier (CMR). Our results are consistent with: (*a*) The capacitance shows increase for values lower and greater than *a specific value* (*from* −1.5 V *and* 0.9 V) provoking *on* switch state in the device without gate current; (*b*) diffusion [depletion] capacitance is present under forward and reverse [only reverse] bias; (*c*) a rectifier with asymmetric bi-directional bias is acquired; (*d*) also the CMR device has the same capacitive properties of usual thyristor family and Schottky diode integrated in a single device. The CMR could be utilized as a device that works at low potency level and high operational frequencies as PHz, e.g., 10^{12} times higher than typical devices and it could be useful for applications in switches that demand high-speed static pulse signals.

Keywords: Source-Drain-Gate Device, Quantum Mechanics Methodology, Three-Terminal Device.

RESEARCH ARTICLE

1. INTRODUCTION

Since the molecular rectifier proposed by Aviram and Ratner[1] in a paper where a uni-dimensional molecular system with a source (S) attached to Drain (D) by a carbon saturated bridge (σ bonds) presenting strong current rectification works have been done. One of them made by Schoonveld and collaborators[2] where organic thin-film transistors have been made to investigate the electronic transport ability in circuits. They found out that the effects provoked by capacitance should be carefully addressed resulting a direct connection of the conductivity and the intrinsic nearest-neighbor tunnel resistance and the capacitance of the individual molecules. Also, in well-ordered structures as single electron characteristics presenting quantized capacitance charging in a nano-electronic switch have been investigated.[3]

Likewise, several experimental works have been done addressing capacitive properties of organic nanodevices. For instance as the investigation of capacitive coupling between the gate and pentacene, it permits the use of voltages under 2 V to modulate the current by 10^4 (Ref. [4]) {10^5 (Refs. [5, 6])} presenting a linear regime and hole mobilities of 0.01 cm^2 $(V\ s)^{-1}$ (Ref. [4]) {120 cm^2 $(V\ s)^{-1}$ (Refs. [5, 6])}. Also, within low operational voltages, it has been demonstrated that the threshold changes due the passivation of surface states of film. This was important to rise up few applications in logic circuits that need high-performance inverters with depletion loads.[7] Using an amorphous molecular gate dielectric it is possible by self-assembly methodology produces a device (gate dielectric) a thickness of 2.5 nm providing a gate capacitance near 1 μF cm^{-2} and low voltage showing low gate current densities equal to 10^{-9} A cm^{-2}.[8]

With a voltage higher than 3 V, it is possible to store energy up to 25 eV in a system composed by gold nanoparticles and a conductive substrate using a bi-functional monolayer of an organic molecule.[9] In the other way, this device will have a full discharge in an electric circuit slower than 1.5 GHz.[9]

Beside the fact that several *organic* devices were investigated concerning a dielectric signature of gate terminal[10–12] presenting a few rules to investigate trap states, there is a few different types of capacitive effects that changes the carrier transport;[13–18] in simple words, mobility and charge density are ruled by: (a) the electronic mobility has not a dependence with the number of groups attached; (b) the molecular structure presents *trans* ↔ *cis* modification could

*Author to whom correspondence should be addressed.

be utilized as molecular gate; (c) the carrier accumulation is inversely dependent of length when conjugated rings are attached with molecular radicals; (d) occurrence of structural deformation as soliton, polaron or bipolaron in the backbone of the structure.

Recently, it raised up that molecular systems have competitive effects between diffusive and ballistic conduction and understanding these capacitive properties should be addressed and controlled in nano-scale.[19] In the present work we investigate by quantum mechanics calculations the capacitive properties of organic three-terminal devices (Fig. 1). In the next section, the system and methodology utilized and the results and conclusions will be presented in the last two sections.

2. SYSTEM AND METHODOLOGY

We investigate a 3-terminal device with the intention to reach out new transport properties unobserved in macro devices or two-terminal nano-devices. This signature could be followed by the quantum nature of organic structure as a single electronic compound and as Non-ohmic behavior for molecular electronic devices. It has been recently addressed[20] showing nonlinear voltage–current characteristic as an intrinsic organic thyristor. The molecular structure of controlled molecular rectifier (CMR) is showed in Figure 1 (*Left*).

Hartree-Fock (HF) approaches contained in Gaussian package[21] was employed including standard basis sets were used for all calculations performing the same qualitative results. The geometric forms of the analyzed structures were fully optimized using HF methodology including a Voltage as an external electrical field in form of Roothaan-Hall matrix in a model within closed shell.

The methodology presented here is based on the same grounds used in successful model presented elsewhere.[22, 23] This is a general procedure to study nanostructured systems and it is a competitive technique compared with other ones[24, 25] utilized in materials engineering design such as that involving the quantum transportation. This is the first theoretical simulation of capacitive effects in an idealized organic 3-terminal prototype nanodevice. Also, we would like to stress that this procedure is not depending on specific parameters or empirical values. It is based on first principle quantum mechanics calculations.

3. RESULTS AND DISCUSSION

Fundamentally, usual devices can have two capacitive effects for high frequencies: depletion (or transition) and diffusion (or accumulation) capacitance. Under reverse and forward polarization occur the transition (Ct) and diffusion (Cd) capacitances, respectively. When the device is under a reverse polarization, the depletion region increases with the reverse potential and decreases the transition capacitance. In the opposite way, for forward polarization, the capacitance is dependent of injected carriers for the outside depletion regions, e.g., it depends on main carriers of the device. Also, high current levels have a dependence of high diffusion capacitance level.

Henceforth, in the molecular level the capacitive effects are different but the concept remains correct and it has the validation as a way to describe the charge in the interface molecule-electrode. Iafrete et al.[26] propose in molecular level the capacitance as:

$$C(N) = \frac{e^2}{IP(N) - EA(N)} \tag{3}$$

for a closed shell system with N-electrons, where the ionization potential ($IP(N)$) and the electro-affinity ($EA(N)$) should be take into account.

The molecular capacitance is a function of number of electrons in the system, in opposite way of usual capacitors that depends of its own liquid charge distribution over the device shape.

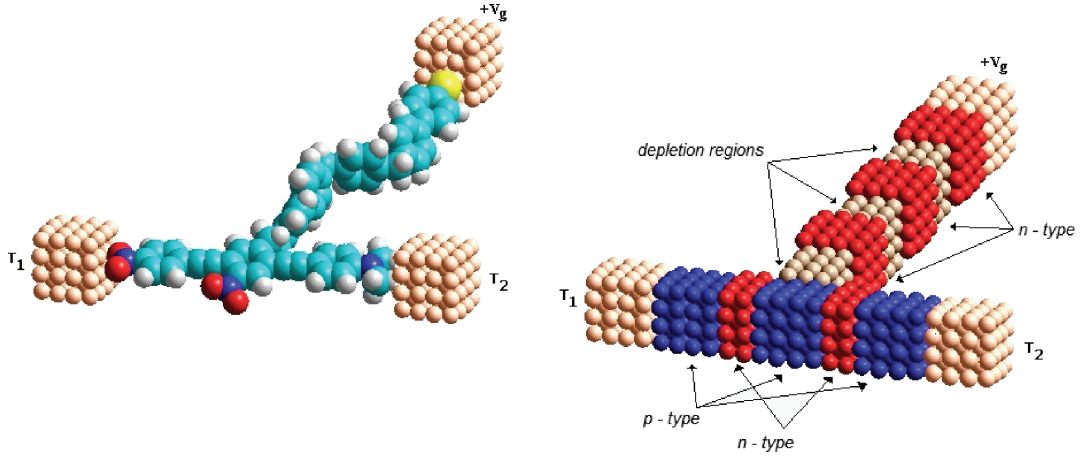

Fig. 1. Pictogram of Controlled Molecular Rectifier (CMR): (*Left*) Horizontally the device presenting the gate molecular structure composed by a conjugated polymer separated by aliphatic CH_2 atoms and almost vertically (connected to +Vg) the main rectifier molecule within donor and acceptor groups attached in the extremities; (*Right*) Pictorial analogy with usual devices including *p–n* semiconductor junctions and depletion regions.

RESEARCH ARTICLE

In Figure 1, it presents a pictogram representing the molecular structure calculated in this work as well as a semiconductor model presenting *p–n* junctions. The calculated nanodevice obtained (left) was represented by *p* and *n* regions as usual semiconductor devices do. Following the majority carrier it is possible to identify the class of clusters as well as the depletion region that permits the device works as semiconductor device (right). These depletion regions found in the molecular gate composed by CH_2 aliphatic groups and they are responsible for the quantum wells in the system. However, for a $+\mathbf{V}_g$, the majority carriers by drift current provoke the *p* region doping increasing the number of carriers (electrons), and depending of direction of applied voltage, it will appear charge diffusion in the same direction of polarization.

In Figure 2, it presents the capacitance versus voltage for the molecular gate of the device. Within the increase of reverse polarization, the charge accumulation in the gate abruptly decreases due the increase of molecular quantum well, e.g., increasing of the depletion region. We observe that appears a transition capacitance by charge accumulation in the lowest unoccupied molecular orbitals while decrease under reverse bias. However, for forward bias appears tunneling of majority carriers through the quantum wells, which are undesirable for any capacitor. The variation of transition capacitance at reverse bias can be utilized as a usual varactor diode (variable voltage capacitor).

In Figure 3, it presents the capacitance versus voltage for the main molecule of the device. The main molecule is in the *off* state between −3.5 V and 2.0 V and it mainly presents depletion capacitance by majority carriers from the π-orbitals in the extremities of molecular terminals (T_1 and T_2). In the *on* state (under forward and reverse bias) presents charge increase by diffusion in the main molecule implying in high diffusion capacitance.

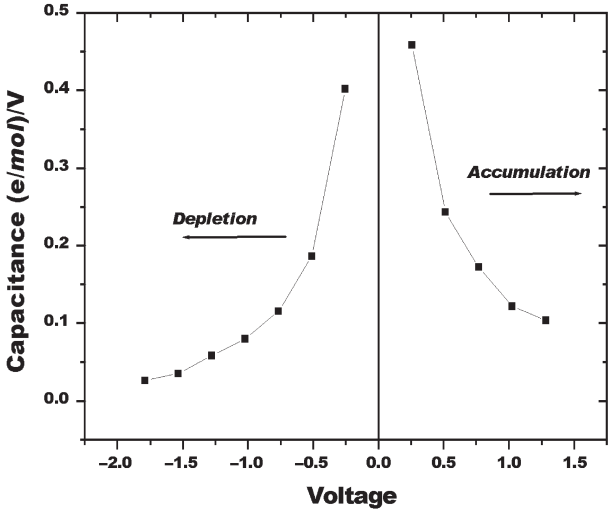

Fig. 2. *Capacitance–Voltage* for the CMR investigated applying an external electrical field in gate terminal (Represented by $\mathbf{V}_g$ in Fig. 1).

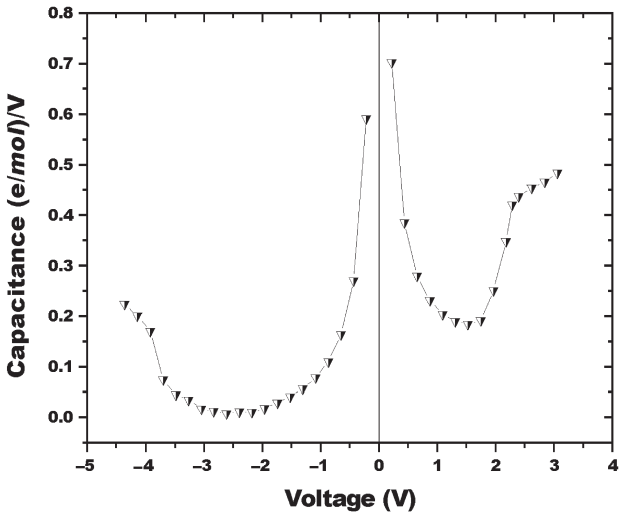

Fig. 3. *Capacitance–Voltage* for positive applied bias in T_1–T_2 terminals represented in Figure 1.

In Figure 4, it presents the theoretical absorption spectra by HF methodology including configuration interaction to give the best description of the UV-Visible-IR optical transitions and taken into account from the first 12 unoccupied molecular orbitals to the last 12 occupied molecular orbitals, including singlet states. Figure 4(a) shows three main bands centered at 188 nm, 258 nm and 337 nm composed by transitions presented in the figure. The molecular system under a reverse {Fig. 4(b), see the representation of −3.5 V in Fig. 3} and forward {Fig. 4(c), see the representation of 1.8 V in Fig. 3} bias rose up a *very important* pattern: When the voltage goes to the operational *on* switch, a strong red shift of main transitions appears composed

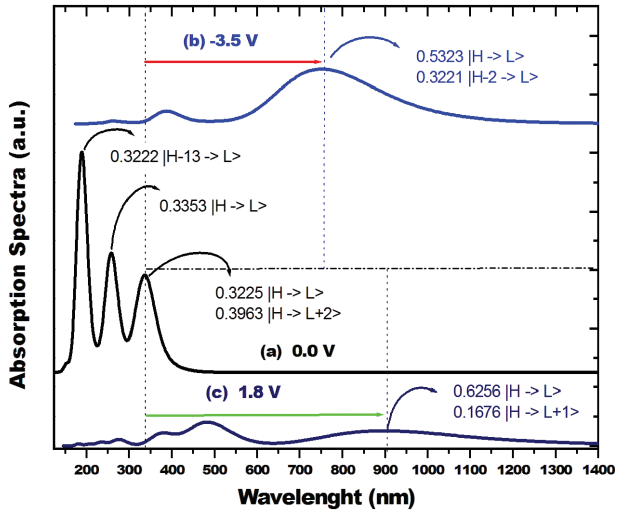

Fig. 4. Theoretical absorption spectra of CMR device for (a) 0.0 V, (b) −3.5 V and (c) 1.8 V applied bias. The **H** and **L** means the Highest occupied molecular orbital and the Lowest unoccupied molecular orbital, respectively. The $A|\mathrm{H}-x \rightarrow \mathrm{L}+y\rangle$ is a representation of a HOMO minus x to LUMO plus y molecular transition weighted by the A coefficient of LCAO (linear combination of atomic orbitals) expansion.

RESEARCH ARTICLE

mainly by orbitals close to material gap and provoking a squeezed gap.

Also, in Schottky diode, we can obtain the capacitance as a function of the applied voltage by taking the derivative of the

$$C_j = \left|\frac{dQ_d}{dV_a}\right| = \sqrt{\frac{q\varepsilon_s N_d}{2(\phi_i - V_a)}} = \frac{\varepsilon_s}{x_d} \quad (4)$$

where ε_s is the semiconductor dielectric constant and also is assumed full ionization implying the ionized donor density equals the donor density, N_d. The last term in the equation indicates that the expression of a parallel plate capacitor still applies. We can understand this once one realizes that the charge added {removed} from the depletion layer as one decreases {increases} the applied voltage is added {removed} only at the edge of the depletion region. While the parallel plate capacitor expression seems to imply that the capacitance is a constant, the metal–semiconductor junction capacitance is not constant since the depletion layer width, x_d, varies with the applied voltage.

For completeness, in comparison with CMR device, the Figure 5 is presented the Thyristor device composed by four *pnpn* layers and three serial junctions: **J1**, **J2** e **J3**. The Schottky contact (Sc) in the first *p* layer is called as anode (A) and the metal-semiconductor contact with the *n* layer is called as cathode (K). Three main behaviors can be denoted:

(a) For reverse polarization (blockage reverse), the **J2** junction is directly polarized;

(b) Instead **J1** and **J3** are inversely polarized creating diffusion and transition capacitances in the junctions, respectively;

(c) Under forward polarization implies all three junctions directly polarized increasing the transport of the device and consequently raising the diffusion capacitance.

The CMR has three Schottky junctions in the **T1**, **T2** and **G** terminals and five semiconductor-*like* layers *pnpnp* (Note in Figs. 1 and 5). It is reduced in only three *pnp* layers when the central aromatic ring within NO_2 attached receive the majority carrier flow from the gate terminal (molecule) provoking a large *n*-type layer resulting in two **J1*** and **J2*** layers forward polarized.

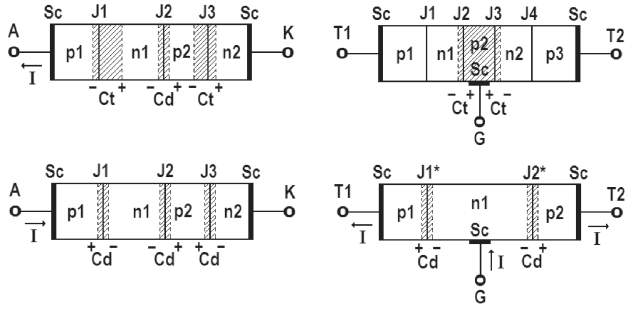

Fig. 5. In left panel, depletion layer widths and voltage drops of usual thyristor operated under reverse blocking and forward conducting, up and down, respectively. In right panel, show one-dimensional cross section of the *CMR* nanodevice, when electrons are injected into $n1$-base region, lowering its resistivity and resulting in a low-voltage drop. This is the *on*-state of the nanodevice.

Also, it is well-known that for the design of semiconductor devices the calculation of the rectification ratio[27] representing the ratio between the current at a positive bias V divided by absolute value of the current at the corresponding negative bias −V, e.g., quantification and qualification of the device working as rectifier. For CMR presented here is equal to **18.37** and considered excellent result for the efficiency of molecular rectifiers.[28, 29]

4. CONCLUSION

In this paper we present theoretical design for the capacitive effects for an organic three-terminal nanodevice. The CMR device has length x width equal to 6.65 nm^2 and presents a gate voltage from *off* to *on* state equal to 1.5 V only (Typical devices presents gate voltage of 30 V). Also, the results have particular characteristics under specifics bias conditions as:

(I) Following the leads of capacitive effects, it is possible to utilize the CMR device as bi-directional rectifier;

(II) Increasing the charge accumulation provokes a switch *on* in the main molecule without gate current (From Figs. 2 and 3 for voltages equal or lower [greater] than −3.5 V [2.0 V]);

(III) It works as Thyristor and Schottky diode devices *in one* integrated under specific bias condition.

Overall, we have showed the design associated with the capacitive effects of an organic three-terminal nanodevice that presents the same capacitive properties found in regular devices (Thyristor and Schottky diode).[22]

Acknowledgment: Marcos Allan Leite Reis and Aldilene Saraiva-Souza are grateful to CAPES and CNPq fellowship, respectively. We would like to thank FAPEsPa for financial support.

References

1. A. Aviram and M. A. Ratner, *Chem. Phys. Lett.* 29, 277 (**1974**).
2. W. A. Schoonveld, J. Wildeman, D. Fichou, P. A. Bobbert, B. J. van Wees, and T. M. Klapwijk, *Nature* 404, 977 (**2000**).
3. D. I. Gittins, D. Bethell, D. J. Schiffrin, and R. J. Nichols, *Nature* 408, 67 (**2000**).
4. M. J. Panzer, C. R. Newman, and C. D. Frisbie, *Appl. Phys. Lett.* 86, 103503 (**2005**).
5. L. Wang, M.-H. Yoon, G. Lu, Y. Yang, A. Facchetti, and T. J. Marks, *Nat. Mater.* 5, 893 (**2006**).
6. L. Wang, M.-H. Yoon, G. Lu, Y. Yang, A. Facchetti, and T. J. Marks, *Nat. Mater.* 6, 317 (**2007**).
7. Y. Choi, I.-D. Kim, H. L. Tuller, and A. I. Akinwande, *IEEE Trans. on Electron Devices* 52, 2819 (**2005**).
8. M. Halik, H. Klauk, U. Zschieschang, G. Schmid, C. Dehm, M. Schutz, S. Maisch, F. Effenberger, M. Brunnbauer, and F. Stellacci, *Nature* 431, 963 (**2004**).

9. M. B. Cortie, M. H. Zareie, S. R. Ekanayake, and M. J. Ford, *IEEE Trans. on Nanotech.* 4, 406 **(2005)**.
10. A. Wang, I. Kymissis, V. Bulovic, and A. I. Akinwande, *IEEE Trans. on Electron Devices* 53, 9 **(2006)**.
11. A. Saraiva-Souza, A. G. Souza Filho, B. G. Sumpter, V. Meunier, and J. D. Nero, *J. Phys. Chem. C* accepted 05/2008.
12. L. S. C. Pingree, M. T. Russell, T. J. Marksa, and M. C. Hersam, *J. Appl. Phys.* 100, 044502 **(2006)**.
13. N. Matsunaga and K. Sohlberg, *J. Nanosci. Nanotechnol.* 1, 275 **(2001)**.
14. N. Radulovic et al., *J. Comput. Theor. Nanosci.* 3, 551 **(2006)**.
15. D. B. de Lima and J. D. Nero, *J. Comput. Theor. Nanosci.* **(2008)**, in press.
16. H. Klauk, U. Zschieschang, J. Pflaum, and M. Halik, *Nature* 4445, 745 **(2007)**.
17. M. Freitag, J. C. Tsang, A. Bol, D. Yuan, J. Liu, and P. Avouris, *Nano Lett.* 7, 2037 **(2007)**.
18. J. D. Nero and C. P. de Melo, *Synth. Met.* 121, 1741 **(2001)**.
19. A. Nitzan, *Science* 317, 759 **(2007)**.
20. F. Sawano, I. Terasaki, H. Mori, T. Mori, M. Watanabe, N. Ikeda, Y. Nogami, and Y. Noda, *Nature* 437, 522 **(2005)**.
21. M. J. Frisch, G. W. Trucks, H. B. Schlegel, G. E. Scuseria, M. A. Robb, J. R. Cheeseman, V. G. Zakrzewski, J. A. Montgomery, Jr., R. E. Stratmann, J. C. Burant, S. Dapprich, J. M. Millam, A. D. Daniels, K. N. Kudin, M. C. Strain, O. Farkas, J. Tomasi, V. Barone, M. Cossi, R. Cammi, B. Mennucci, C. Pomelli, C. Adamo, S. Clifford, J. Ochterski, G. A. Petersson, P. Y. Ayala, Q. Cui, K. Morokuma, D. K. Malick, A. D. Rabuck, K. Raghavachari, J. B. Foresman, J. Cioslowski, J. V. Ortiz, A. G. Baboul, B. B. Stefanov, G. Liu, A. Liashenko, P. Piskorz, I. Komaromi, R. Gomperts, R. L. Martin, D. J. Fox, T. Keith, M. A. Al-Laham, C. Y. Peng, A. Nanayakkara, C. Gonzalez, M. Challacombe, P. M. W. Gill, B. Johnson, W. Chen, M. W. Wong, J. L. Andres, C. Gonzalez, M. Head-Gordon, E. S. Replogle, and J. A. Pople, Gaussian 98, Revision A.7, Gaussian, Inc., Pittsburgh, PA **(1998)**.
22. M. A. L. Reis and J. D. Nero, *J. Comput. Theor. Nanosci.* 5, 567 **(2008)**.
23. D. B. de Lima, M. A. L. Reis, F. M. Souza, and J. D. Nero, *J. Comput. Theor. Nanosci.* 5, 563 **(2008)**.
24. U. Ganguly, C. Lee, T.-H. Hou, and E. C. Kan, *IEEE Trans. Nanotech.* 6, 22 **(2007)**.
25. J. M. Seminario, L. Yan, and Y. Ma, *IEEE Trans. Nanotech.* 5, 436 **(2006)**.
26. G. J. Iafrate, K. Hess, J. B. Krieger, and M. Macucci, *Phys. Rev. B* 52, 10737 **(1995)**.
27. N. W. Ashcroft and N. D. Mermin, Solid State Physics, International Edition, ISBN: 0-03-04934 **(1976)**.
28. I. I. Oleynik, M. A. Kozhushner, V. S. Posvyanskii, and L. Yu, *Phys. Rev. Lett.* 96, 096803 **(2006)**.
29. R. Liua, S.-H. Ke, W. Yang, and H. U. Baranger, *J. Chem. Phys.* 124, 024718 **(2006)**.

Received: 4 June 2007. Accepted: 10 July 2007.